

# Charge and spin excitation spectra in the one-dimensional Hubbard model with next-nearest-neighbor hopping

S. Nishimoto,<sup>1</sup> T. Shirakawa,<sup>2</sup> and Y. Ohta<sup>2,3</sup>

<sup>1</sup>*Max-Planck-Institut für Physik komplexer Systeme, D-01187 Dresden, Germany*

<sup>2</sup>*Graduate School of Science and Technology, Chiba University, Chiba 263-8522, Japan*

<sup>3</sup>*Department of Physics, Chiba University, Chiba 263-8522, Japan*

(Dated: March 16, 2018)

The dynamical density-matrix renormalization group technique is used to calculate spin and charge excitation spectra in the one-dimensional (1D) Hubbard model at quarter filling with nearest-neighbor  $t$  and next-nearest-neighbor  $t'$  hopping integrals. We consider a case where  $t$  ( $> 0$ ) is much smaller than  $t'$  ( $> 0$ ). We find that the spin and charge excitation spectra come from the two nearly independent  $t'$ -chains and are basically the same as those of the 1D Hubbard (and  $t$ - $J$ ) chain at quarter filling. However, we find that the hopping integral  $t$  plays a crucial role in the short-range spin and charge correlations; i.e., the ferromagnetic spin correlations between electrons on the neighboring sites is enhanced and simultaneously the spin-triplet pairing correlations is induced, of which the consequences are clearly seen in the calculated spin and charge excitation spectra at low energies.

PACS numbers: 71.10.Pm, 71.10.Fd, 78.30.Jw, 72.15.Nj, 71.30.+h, 71.45.Lr

## I. INTRODUCTION

Spin-triplet superconductivity has been one of the major issues in the field of condensed-matter physics. Nearly all the conventional and unconventional superconductors known to date are spin-singlet paired. The best-known example of triplet pairing is not a superconductor but a superfluid  $^3\text{He}$ , where atomic Cooper pairs are formed in spin-triplet channel.<sup>1</sup> Only a few materials of spin-triplet superconductivity have so far been confirmed in strongly correlated electron systems, which include ruthenium oxide  $\text{Sr}_2\text{RuO}_4$ <sup>2</sup> and some heavy-fermion compounds such as  $\text{UPt}_3$ .<sup>3</sup> Here, some questions will naturally arise. One is whether the electron correlation can take an essential part in superconductivity carried by spin-triplet pairs. Another is how the behavior differs from that of spin-singlet superconductivity. In this manner, research on spin-triplet superconductivity may offer an opportunity to expose unknown physical phenomena.

Quite recently, a new mechanism of the spin-triplet superconductivity has been proposed in a fairly simple correlated electron system.<sup>4</sup> The model consists of two Hubbard chains coupled with zigzag bonds and has a unique structure of hopping integrals: sign of the hopping integrals changes alternately along the zigzag bonds connecting two chains, while the sign along the one-dimensional (1D) chain is always negative. [A model where all the hopping integrals are taken to be positive is equivalent under canonical transformation.] Under this sign rule of the hopping integrals, the ring-exchange mechanism<sup>5</sup> yields ferromagnetic spin correlations, and accordingly, attractive interaction between electrons is derived. In Ref. 4, the argument was developed on the basis of only the static properties such as pair binding energy, spin excitation gap, and pair correlation function, as well as spin correlation function. Therefore, further investigations including dynamical properties have been

desired.

As for real materials, this mechanism<sup>4</sup> may be of possible relevance to superconductivity observed in quasi-1D organic conductor  $(\text{TMTSF})_2\text{X}$  [ $\text{X}=\text{PF}_6, \text{ClO}_4$ , etc.], the so-called Bechgaard salts.<sup>6,7</sup> The system exhibits a rich phase diagram upon variation of the pressure and temperature. At low temperatures, the phase changes, in the order, as the spin-Peierls insulator, antiferromagnetic insulator, spin-density-wave (SDW) insulator, superconductivity, and paramagnetic metal, with increasing pressure. So far, experimental evidences that the superconducting state occurs in the triplet channel have been piled up,<sup>8</sup> although not much is known on the nature of the pairing. A newly synthesized copper-oxide compound  $\text{Pr}_2\text{Ba}_4\text{Cu}_7\text{O}_{15-\delta}$ <sup>9</sup> may also be a relating system. This material consists of both the single  $\text{CuO}$  chains (as in  $\text{PrBa}_2\text{Cu}_3\text{O}_7$ ) and the double  $\text{CuO}$  chains (as in  $\text{PrBa}_2\text{Cu}_4\text{O}_8$ ), and those chains are separated by insulating  $\text{CuO}_2$  plains. It has been reported that the double chains turn into a superconducting state below  $T_c \sim 10$  K.<sup>10</sup> Although the signs of the hopping integrals seem not to satisfy the ferromagnetic sign rule, the structure of the double  $\text{CuO}$  chains bears a certain similarity to our model.<sup>11</sup>

The purpose of the present study is therefore to build up understanding of the ring-exchange superconducting mechanism by calculating dynamical quantities for the same model proposed in Ref. 4. To see the excitations in the spin and charge degrees of freedom separately, we here calculate the momentum-dependent dynamical spin-spin and density-density correlation functions. We use the dynamical density-matrix renormalization group (DDMRG) method for calculating dynamical quantities,<sup>12</sup> which is an extension of the standard DMRG method.<sup>13</sup> The obtained results with high resolutions enable us to discuss details of the fundamental properties on the spin and charge excitations. Thus,

we can find some interesting features in the low-energy physics of our model.

We will show that, although the spin and charge excitation spectra are basically the same as those of the two weakly-coupled 1D Hubbard (and  $t$ - $J$ ) chains at quarter filling, the small hopping integral between the chains plays a crucial role in the short-range correlations and low-energy excitations; i.e., the ferromagnetic spin correlations between electrons on the neighboring sites is enhanced and the spin-triplet pairing correlations between the electrons is induced, of which the consequences are clearly seen in the calculated spin and charge excitation spectra at low energies. We hope that the present investigation will provide deeper insight into the mechanism of the spin-triplet superconductivity.

Our paper is organized as follows. In Sec. II, we define the 1D  $t$ - $t'$ - $U$  model and introduce the physical quantities of interest, namely, spin and charge excitation spectra. In Sec. III, exact solution of the spin (and charge) excitation spectrum in the noninteracting case is presented, and by comparing our result with the exact one, we evaluate the performance of our DDMRG method. We then study the spectra with onsite Coulomb interaction and discuss relevance to the spin-triplet superconductivity. We close with a summary in Sec. IV.

## II. MODEL AND METHOD

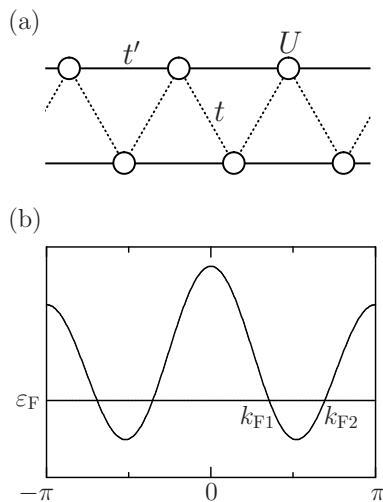


FIG. 1: Schematic representations of (a) the lattice structure of our model and (b) noninteracting band dispersion at  $t'/t > 1$ .

We consider the 1D Hubbard model defined by the Hamiltonian

$$H = t \sum_{i,\sigma} (c_{i+1\sigma}^\dagger c_{i\sigma} + \text{H.c.}) + t' \sum_{i,\sigma} (c_{i+2\sigma}^\dagger c_{i\sigma} + \text{H.c.}) + U \sum_i n_{i\uparrow} n_{i\downarrow}. \quad (1)$$

where  $c_{i\sigma}^\dagger$  ( $c_{i\sigma}$ ) is the creation (annihilation) operator of an electron with spin  $\sigma$  ( $\sigma = \uparrow, \downarrow$ ) at site  $i$ ,  $n_{i\sigma} = c_{i\sigma}^\dagger c_{i\sigma}$  is the number operator,  $t'$  and  $t$  are the nearest-neighbor and next-nearest-neighbor hopping integrals respectively, and  $U$  is the on-site Coulomb interaction. We choose the signs of the hopping integrals  $t$  and  $t'$  to be positive, so that the two spins on a triangle of the lattice align ferromagnetically when  $U$  is large.<sup>4</sup> The lattice structure of our model is shown schematically in Fig. 1(a). We call the chain along the  $t$  ( $t'$ ) hopping integral the  $t$ -chain ( $t'$ -chain). The dispersion relation is given by

$$\varepsilon_k = 2t \cos ka + 2t' \cos 2ka, \quad (2)$$

where  $a$  is the lattice constant along the  $t$ -chain (we set  $a = 1$  hereafter). We consider the case where there are four Fermi momenta  $\pm k_{F1}$  and  $\pm k_{F2}$  ( $|k_{F2}| > |k_{F1}|$ ); i.e., the case where there are two branches in the noninteracting band dispersion [see Fig. 1(b)]. This case occurs when the hopping integrals satisfy the condition

$$\frac{t'}{t} > \frac{\cos^2 [(2-\rho)\pi/2]}{\sin^2 [(2-\rho)\pi]} \quad (3)$$

where  $\rho$  is the band filling. In this paper, we restrict ourselves to the case where  $t'$  is a few times as large as  $t$  and the system is at quarter filling,  $\rho = 1/2$ . Hence, the model can be regarded as a double  $t'$ -chain Hubbard model weakly coupled by the  $t$ -chain.

Because  $t$  is much smaller than  $t'$ , it would be very useful to allow a case of  $t = 0$  for familiarization with our results. In the limit of  $t \rightarrow 0$ , the system is equivalent to the two independent 1D Hubbard chains at quarter filling since electrons are distributed equally to the two chains. The noninteracting band dispersion reads  $\varepsilon_k = 2t' \cos 2k$  and there are four Fermi momenta  $\pm k_{F1} = \pm 5\pi/8$  and  $\pm k_{F2} = \pm 3\pi/8$  in the original Brillouin zone defined for the  $t$ -chain. We define  $2k_F^* = k_{F2} - k_{F1} = \pi/4$  as the ‘nesting’ vector in our model at  $t = 0$ . We use this definition of the Brillouin zone throughout the paper.

We calculate the spin excitation spectrum

$$S(q, \omega) = \frac{1}{\pi} \text{Im} \langle \Psi_0 | s_q^+ \frac{1}{\hat{H} + \omega - E_0 - i\eta} s_{-q}^- | \Psi_0 \rangle, \quad (4)$$

defined with  $s_q^+ = (1/\sqrt{L}) \sum_r e^{iqr} c_{r\uparrow}^\dagger c_{r\downarrow}$ , and the charge excitation spectrum

$$N(q, \omega) = \frac{1}{\pi} \text{Im} \langle \Psi_0 | n_q \frac{1}{\hat{H} + \omega - E_0 - i\eta} n_{-q} | \Psi_0 \rangle, \quad (5)$$

defined with  $n_q = (1/\sqrt{L}) \sum_{r\sigma} e^{iqr} n_{r\sigma}$ . Here,  $|\Psi_0\rangle$  and  $E_0$  are, respectively, the wavefunction and energy of the ground state of the Hamiltonian Eq. (1). The DDMRG technique is applied to calculate the excitation spectra. We here use the open-end boundary condition (OBC) for accurate calculation, because the system is relatively hard to deal with by the DMRG method due to large long-range hopping integrals.<sup>13</sup> When the OBC is used,

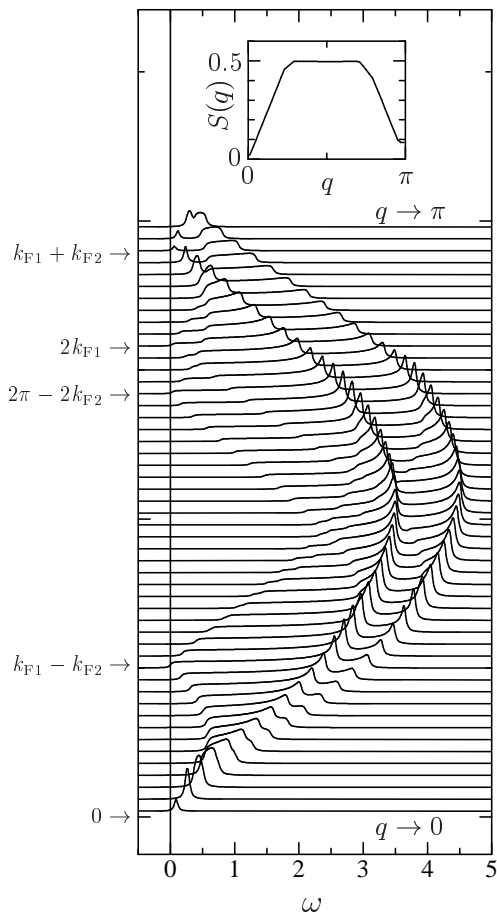


FIG. 2: Exact spin excitation spectrum  $2S(q, \omega)$  [ $= N(q, \omega)$ ] for  $t = 0.25$  and  $t' = 1$  in the noninteracting case ( $U = 0$ ). Broadening of the spectrum  $\eta = 0.03$  is introduced. Five momenta indicated with arrows in the left side denote gapless points. Inset: Exact spin structure factor  $S(q)$ .

we need to use the quasimomenta  $k = \pi m / (L + 1)$  for integers  $1 \leq m \leq L$  on a chain with  $L$  sites in order to express the momentum-dependent operators  $s_q^\pm$  and  $n_{q\sigma}$ .<sup>14</sup>

### III. RESULTS

#### Noninteracting spectrum

First, let us consider the noninteracting case,  $U = 0$ , where the model is exactly solvable. In this case, an excitation corresponds to creating a particle-hole pair for the ground state and therefore we can obtain the exact spectrum of spin excitations:

$$S(q, \omega) = \lim_{\eta \rightarrow +0} \frac{1}{\pi L} \sum_{\varepsilon_k < \varepsilon_F < \varepsilon_{k+q}} \frac{\eta}{(\omega - \varepsilon_{k+q} + \varepsilon_k)^2 + \eta^2} \quad (6)$$

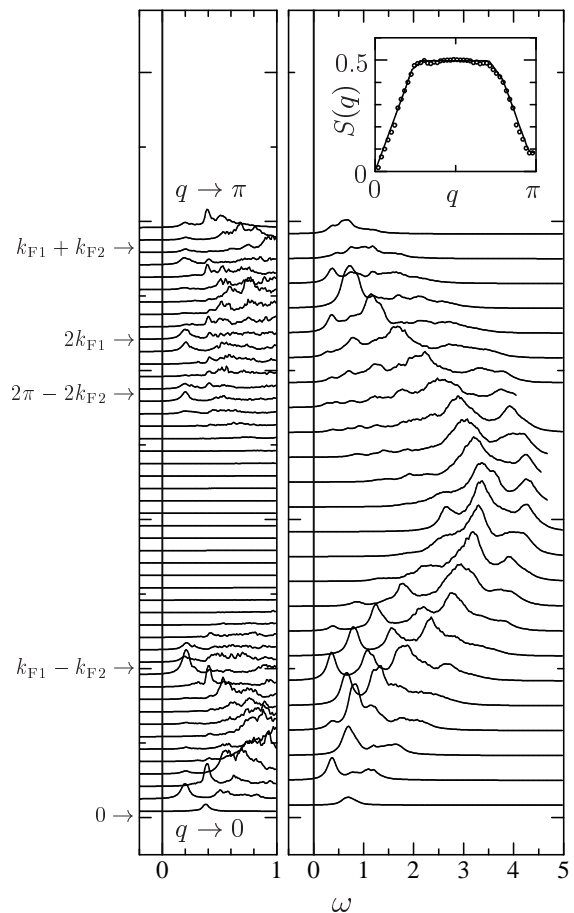


FIG. 3: Spin excitation spectrum  $2S(q, \omega)$  [ $= N(q, \omega)$ ] in the noninteracting case ( $U = 0$ ) calculated by the DDMRG method. The same set of the parameter values as in Fig. 2 is used. Right (left) panel shows the result for  $L = 24$  and  $\eta = 0.1$  ( $L = 48$  and  $\eta = 0.04$ ). Inset: Spin structure factor  $S(q)$  obtained from  $\omega$ -integration of  $S(q, \omega)$ .

where small  $\eta$  is introduced to regularize the poles at particular frequencies  $\omega$ . Note that the spectrum of charge excitations at  $U = 0$  is exactly twice as large as that of the spin excitations, i.e.,  $N(q, \omega) = 2S(q, \omega)$ , because  $N(q, \omega)$  is just a sum over both up and down spins.

In Fig. 2, we show the exact noninteracting spin excitation spectrum  $S(q, \omega)$  given in Eq. (6). For small  $t/t' (< 1)$ , the spectrum contains two predominant features: (i) large-weighted structure consisting of the double sine curve, whose dispersions are approximately written as  $\omega \sim (4t' \pm 2t) \sin q$ , and (ii) small-weighted continuum structure at low frequencies, which arises from excitations between different branches of the noninteracting bands. A zero-energy excitation is caused by the creation of a particle-hole pair just at the Fermi level  $\varepsilon_F$ , so that the gap closes at five momenta  $q = 0$ ,  $k_{F2} - k_{F1}$  ( $= \pi/4$ ),  $2k_{F1}$ ,  $2k_{F1}$ , and  $k_{F1} + k_{F2}$ .

Now, using the DDMRG method, we attempt to reproduce the noninteracting spin excitation spectrum. The

result is shown in Fig. 2. Since the noninteracting model poses a nontrivial problem to the DDMRG technique, it gives us a relevant accuracy test. When carrying out the DDMRG calculation, we have to take into account the required CPU time. Usually, the DDMRG method takes much longer CPU time than the standard DMRG method because the excited states must be obtained and an asked quantity must be calculated (almost) individually for each frequency. Additionally, a required CPU time  $\tau_{\text{CPU}}$  increases rapidly with frequency  $\omega$  and system size  $L$  in the DDMRG calculation, which is estimated approximately as  $\tau_{\text{CPU}} \propto \omega^\alpha$  ( $1 < \alpha < 2$ ) and as  $\tau_{\text{CPU}} \propto L$  if we keep other conditions. Hence, it would be efficient to take a relatively small system for obtaining an overview of the spectrum and a larger system for studying the detailed structure at low frequencies.

Let us then check our DDMRG result with the exact spectrum. In the right panel of Fig. 3, we show the spin excitation spectrum  $S(q, \omega)$  at  $U = 0$  calculated with the DDMRG method in a chain with  $L = 24$  sites. The structure of the double sine curve can be clearly seen. However, it is hard to see dispersive structures in the continuum spectra at low frequencies because only discrete peaks can be obtained due to the finite-size effect. We need to take larger systems to resolve this problem since the resolution of spectrum can be improved in proportion to the system size. We therefore choose to double the system size,  $L = 48$ , and consider the low-energy excitations. The result is shown in the left panel of Fig. 3. The resolution is obviously improved and we can now confirm the five momenta at which the zero-energy excitations occur. Moreover, we can see good agreement in the spin structure factor  $S(q) [= \sum_\omega S(q, \omega)]$  between the DDMRG and exact results, as shown in the inset of Fig. 3. Thus, we are confident that our DDMRG method indeed enable us to study the detailed structures of the relatively complicated spectrum.

For the information, we keep  $m = 400$  (800) density-matrix eigenstates to obtain the spectrum for  $L = 24$  (48) sites. Note that a larger  $m$  value should be necessary to get the true ground state and excited state  $s_{-q}^- |\Psi_0\rangle$  (or  $n_{-q} |\Psi_0\rangle$ ) of the system. We therefore set  $m = 1200$  in the first 4 – 5 DDMRG sweeps.

### Spin excitation spectrum

Next, let us see how the spin excitation spectrum is modified by the inclusion of the onsite Coulomb interaction  $U$ . In Fig. 4, we show our DDMRG result for the spin excitation spectrum  $S(q, \omega)$  at  $t = 0.25$ ,  $t' = 1$ , and  $U = 10$ , where we use the clusters with  $L = 24$  (right panel) and  $L = 48$  (left panel).

Roughly speaking, the lower edge of the spectrum consists of three sine curves with four nodes at  $q \sim 0$ ,  $k_{\text{F}2} - k_{\text{F}1}$  ( $= \pi/4$ ),  $\pi - (k_{\text{F}2} - k_{\text{F}1})$  ( $= 3\pi/4$ ), and  $\pi$ . The excitation gap seems to close around these nodes. This is consistent with previous theoretical studies,<sup>4,15</sup> which

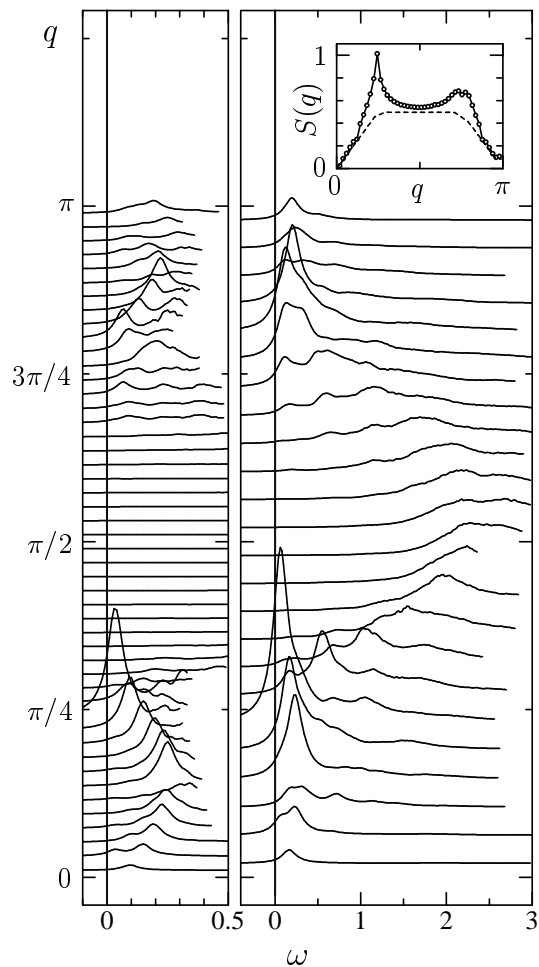


FIG. 4: Spin excitation spectrum  $S(q, \omega)$  at  $t = 0.25$ ,  $t' = 1$ , and  $U = 10$  calculated by the DDMRG method. We use the clusters  $L = 24$  with the broadening  $\eta = 0.1$  (right panel) and  $L = 48$  with  $\eta = 0.04$  (left panel). Inset: Spin structure factor  $S(q)$  obtained from  $\omega$ -integration of  $S(q, \omega)$ .

have suggested that no spin gap exists in the strong coupling regime. On the other hand, the higher edge of the spectrum is approximately represented as a sine curve  $\omega \sim \sin q$  as in the case of  $U = 0$ , which comes from the creation of the particle-hole pairs within the same branch.

Let us now take a closer look at the spectrum. As far as the spin degrees of freedom are concerned, the model Eq. (1) for large  $U$  may be mapped onto a two-chain  $t$ - $J$  model coupled with zigzag bonds. For small  $t/t'$ , the antiferromagnetic interaction along the  $t'$ -chain,  $J'$ , must be much larger than that along the  $t$ -chain,  $J$ , if we assume that the exchange interaction comes from the second-order perturbation of the hopping integrals with a fixed  $U$ , i.e.,  $J' (\sim t'^2) \gg J (\sim t^2)$ . Consequently, the features of the spectrum can be basically interpreted as those of the 1D quarter-filled  $t$ - $J$  model.<sup>17,18,19</sup> The nodes at the lower edge of the DDMRG spectrum occur

at the momenta  $q = 0$ ,  $2k_F^*$ ,  $2\pi - 2k_F^*$ , and  $\pi$ . Also, we can see considerable enhancement of spectral intensities around  $q = \pi/4$  ( $= k_{F2} - k_{F1}$ ) in comparison with the noninteracting spectrum. This indicates that the onsite Coulomb interaction enhances the antiferromagnetic correlation with a period of 4 times the lattice constant along the  $t'$ -chain, which can be easily expected from the fact that the  $2k_F^*$ -SDW correlation is the most dominant for small  $J$  in the 1D  $t$ - $J$  model at quarter filling. This result may be compared with the  $2k_F$ -SDW state observed experimentally in (TMTSF) $_2$ X.<sup>16</sup>

We then examine the effects of a small hopping integral  $t$ , which leads to the antiferromagnetic interaction  $J$  along the  $t$ -chain as mentioned above. From the viewpoint of the spin degrees of freedom, magnetic frustration must be brought because triangular lattices are formed of only the antiferromagnetic interactions. Although  $J$  is much smaller than  $J'$ , we can clearly see the influence in our DDMRG spectrum; there are two nodes around  $q = 3\pi/4$ , i.e.,  $q \sim 2k_{F1}$  ( $> 3\pi/4$ ) and  $2\pi - 2k_{F2}$  ( $< 3\pi/4$ ). These nodes are collected into a single node at  $q = 3\pi/4$  when  $t = 0$ . This split actually signifies a tendency to a formation of the  $2k_F$ -SDW state along the  $t$ -chain as well as to a collapse of the  $2k_F$ -SDW state along the  $t'$ -chain. With increasing  $t/t'$ , the node at  $q = 2k_{F2}$  approaches  $q = \pi/2$  and the adjacent spectral weight increases, whereas the node at  $q = 2k_{F1}$  goes away from  $q = 3\pi/4$  and the weight goes to zero. In other words, the hopping term  $t$  weakens the  $2k_F$ -SDW oscillation along the  $t'$ -chain since the competing antiferromagnetic correlation along the  $t$ -chain is enhanced. In fact, the spectral weight around  $q = \pi/4$  will certainly diminish as  $t/t'$  increases.

Another noticeable feature is that the spectral weight around  $q = 3\pi/4$  is obviously smaller than that around  $q = \pi/4$ , while the spectrum should be symmetrical about  $q = \pi/2$  in the case of  $t = 0$ . This result implies the presence of ferromagnetic spin fluctuations at low energies. For clearer understanding, we study the spin structure factor  $S(q)$ . As shown in the inset of Fig. 4, it is evident that  $S(q)$  around  $q = \pi/4$  is greater than that around  $q = 3\pi/4$ ; otherwise,  $S(q)$  should be almost symmetrical about  $q = \pi/2$ . This result indicates an enhancement of the ferromagnetic spin correlation between the neighbouring sites along the  $t$ -chain. We may explain this as follows.

A real-space behavior of the spin-spin correlation may be derived from the Fourier transform of  $S(q)$ ,

$$\langle S_i^z S_j^z \rangle = \frac{1}{L} \sum_q S(q) e^{iq(r_i - r_j)}, \quad (7)$$

with  $S_i^z = (n_{i\uparrow} - n_{i\downarrow})/2$ . We find that the spin correlation along the  $t'$ -chain is not affected so much by a small  $t$  value but the decay length of the  $2k_F$ -SDW oscillation is slightly shortened. On the contrary, the  $t$  hopping term plays a prominent role in spin correlation between the

$t'$ -chains, which may be estimated as

$$\langle S_i^z S_{i+R}^z \rangle \propto \cos [(\pi/4)R] \times (\text{decaying term}), \quad (8)$$

where  $R$  is an odd number. For  $R = 1$ , we obtain  $\langle S_i^z S_{i+1}^z \rangle = 0.00745$ , which indicates the presence of ferromagnetic correlation between two electrons at the neighboring sites. This result is consistent with a scenario of spin-triplet superconductivity where the pairing of electrons occurs between the inter  $t'$ -chain nearest-neighbor sites, which is proposed in Ref. 4.

### Charge excitation spectrum

Finally, we study the charge correlation function in the presence of the onsite Coulomb interaction  $U$ . In Fig. 5, we show the charge excitation spectrum  $N(q, \omega)$  at  $t = 0.25$ ,  $t' = 1$ , and  $U = 10$ , calculated by the DDMRG method for the chains with  $L = 24$  (right panel) and with  $L = 48$  (left panel). The outline of the spectrum, which is roughly expressed as  $\omega \approx 4t' \sin q$ , seems to be similar to that in the noninteracting spectrum. This result reflects the fact that the overall dispersion is hardly affected by the onsite Coulomb interaction. However, we notice that two distinct features emerge in the low-frequency range of the spectrum, which are discussed below.

One is the increase in the low-energy spectral weight around  $q = \pi/2$  in the excitation spectrum. The excitation gap seems to close there, so that the lower edge of the spectrum consists of the two sine curves with three nodes at  $q \sim 0$ ,  $\pi/2$ , and  $\pi$ . We may thus have one gapless charge mode. This result reflects a tendency toward the Peierls instability, i.e., the formation of the  $4k_F$ -charge-density-wave (CDW) along the  $t'$ -chain. We find that the spectral weight for the  $2k_F$ -CDW correlation is instead much reduced. This feature would be more evident if we observe the momentum-dependent charge structure factor  $N(q)$ , which is shown in the inset of Fig. 5. We find that  $N(q)$  takes the maximum value at  $q = \pi/2$  and goes down along the practically straight lines to  $q = 0$  and  $\pi$ . This dependence is consistent with results in the 1D quarter-filled Hubbard chain at large  $U$ .<sup>20</sup>; in fact, the result is almost equivalent to the result for noninteracting spinless fermions at half filling, as far as the charge degrees of freedom are concerned.

The other is the appearance of large-weighted sharp peaks around  $q = 0$  at  $\omega \approx 0$ . The point is as follows; the spectral weight of the peaks around  $q = 0$  is larger than that around  $q = \pi$  in the low-frequency range, and they are also gathered at lower frequencies. This implies that the electrons tend to come in the neighboring sites along the  $t$ -chain, which is associated with the pairing of two electrons between the inter  $t'$ -chain sites; accordingly, the pairs tend to be arranged alternately along the  $t'$ -chain. Note that the two momenta  $q = 0$  and  $\pi$  should be equivalent when  $t = 0$ , so that the present result implies that the small hopping integral  $t$  enhances the pairing fluctuations at low energies.

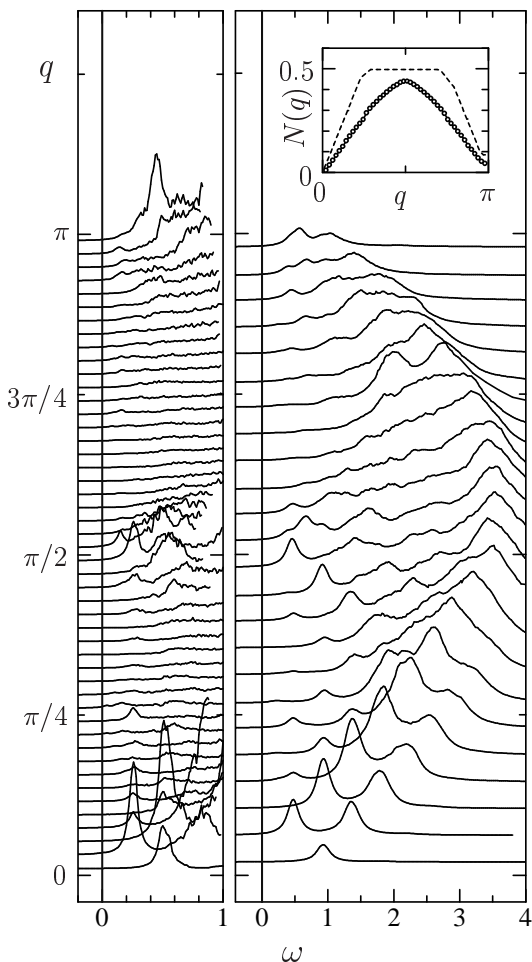


FIG. 5: Charge excitation spectrum  $N(q, \omega)$  calculated by the DDMRG method for the same set of the parameter values as in Fig. 4. We use the clusters  $L = 24$  with broadening  $\eta = 0.1$  (right panel) and  $L = 48$  with  $\eta = 0.04$  (left panel). Inset: Charge structure factor  $N(q)$  obtained from  $\omega$ -integration of  $N(q, \omega)$ .

Additionally, we can estimate the so-called Tomonaga-Luttinger liquid parameter  $K_\rho$  from the derivative of  $N(q)$  at  $q = 0$ ,

$$K_\rho = \frac{\pi}{2} \left. \frac{dN(q)}{dq} \right|_{q=0}, \quad (9)$$

whereby we find the value  $K_\rho \approx 0.637$ . Because, in the presence of one gapless charge mode, the pairing correlation is dominant in comparison with the  $4k_F$ -CDW correlation when  $K_\rho > 0.5$ ,<sup>21,22</sup> our estimated value of  $K_\rho$  is consistent with the occurrence of spin-triplet superconductivity proposed in Ref. 4.

#### IV. SUMMARY

We have calculated the spin and charge excitation spectra of the two-chain zigzag-bond Hubbard model at quarter filling in order to seek for consequences of the spin-triplet pairing induced by the ring-exchange mechanism. The model is topologically equivalent to the 1D Hubbard model with nearest-neighbor  $t$  ( $> 0$ ) and next-nearest-neighbor  $t'$  ( $> 0$ ) hopping integrals. We here have considered the case at  $t \ll t'$ . We have used the DDMRG technique to calculate the excitation spectra.

We have first demonstrated the accuracy of the DDMRG method by reproducing the noninteracting exact spectrum. We have suggested that, for practical calculations, it is necessary to adopt a relatively small system for obtaining an overview of the spectrum and a larger system for investigating detailed structures of the spectrum at low frequencies because the required CPU time increases rapidly with increasing the frequency and/or system size. Thus, the DDMRG method enables us to study the details of relatively complicated structures of the spectra.

Then, we have investigated how the spectra are deformed when the strong onsite Coulomb interaction  $U$  sets in. We find that the spin and charge excitation spectra are basically the same as those of the 1D Hubbard (and  $t$ - $J$ ) chain at quarter filling; i.e., the spectra come from the two nearly independent 1D chains where the  $2k_F$ -SDW and  $4k_F$ -CDW correlations along the  $t'$ -chains are enhanced. However, we find that the hopping integral  $t$  plays a crucial role in the short-range spin and charge correlations; i.e., the ferromagnetic spin correlations between electrons on the neighboring sites is enhanced and the spin-triplet pairing correlations between the electrons is induced, of which the consequences are clearly seen in the calculated spin and charge excitation spectra at low energies. Our DDMRG calculations for the spin and charge excitation spectra have thus supported the ring-exchange mechanism for spin-triplet superconductivity where the pairing of electrons occurs between the two chains.

#### Acknowledgments

We thank T. Takimoto for useful discussions. This work was supported in part by Grants-in-Aid for Scientific Research (Nos. 18028008, 18043006, and 18540338) from the Ministry of Education, Science, Sports, and Culture of Japan. A part of computations was carried out at the Research Center for Computational Science, Okazaki Research Facilities, and the Institute for Solid State Physics, University of Tokyo.

<sup>1</sup> A. J. Leggett, Rev. Mod. Phys. **47**, 331 (1975).

<sup>2</sup> Y. Maeno, H. Hashimoto, K. Yoshida, S. Nishizaki, T. Fu-

- jita, J. G. Bednorz, and F. Lichtenberg, *Nature* **372**, 532 (1994).
- <sup>3</sup> R. Joynt and L. Taillefer, *Rev. Mod. Phys.* **74**, 235 (2002).
- <sup>4</sup> Y. Ohta, S. Nishimoto, T. Shirakara, and Y. Yamaguchi, *Phys. Rev. B* **72**, 012503 (2005).
- <sup>5</sup> P. Fazekas, *Lecture Notes on Electron Correlation and Magnetism* (World Scientific, Singapore, 1999), p. 435.
- <sup>6</sup> D. Jérôme, A. Mazaud, M. Ribault, and K. Bechgaard, *J. Phys. (France) Lett.* **41**, L95 (1980).
- <sup>7</sup> K. Bechgaard, K. Carneiro, M. Olsen, F. B. Rasmussen, and C. S. Jacobsen, *Phys. Rev. Lett.* **46**, 852 (1981).
- <sup>8</sup> I. J. Lee, S. E. Brown, and J. Naughton, *J. Phys. Soc. Jpn.* **75**, 051011 (2006) and references therein.
- <sup>9</sup> M. Matsukawa, Y. Yamada, M. Chiba, H. Ogasawara, T. Shibata, A. Matsushita, and Y. Takano, *Physica C* **411**, 101 (2004).
- <sup>10</sup> S. Sasaki, S. Watanabe, Y. Yamada, F. Ishikawa, K. Fukuda, S. Sekiya, *cond-mat/0603067*.
- <sup>11</sup> K. Sano, Y. Ōno, and Y. Yamada, *J. Phys. Soc. Jpn.* **74**, 2885 (2005).
- <sup>12</sup> E. Jeckelmann, *Phys. Rev. B* **66**, 045114 (2002).
- <sup>13</sup> S. R. White, *Phys. Rev. Lett.* **69**, 2863 (1992); *Phys. Rev. B* **48**, 10345 (1993).
- <sup>14</sup> H. Benthien, F. Gebhard, and E. Jeckelmann, *Phys. Rev. Lett.* **92**, 256401 (2004).
- <sup>15</sup> S. Daul and R. M. Noack, *Phys. Rev. B* **58**, 2635 (1998).
- <sup>16</sup> For a review article, see T. Ishiguro, K. Yamaji, and G. Saito, *Organic Superconductors* (Springer-Verlag, Berlin, 1990).
- <sup>17</sup> P. A. Bares and G. Blatter, *Phys. Rev. Lett.* **64**, 2567 (1990).
- <sup>18</sup> T. Tohyama, P. Horsch and S. Maekawa, *Phys. Rev. Lett.* **74**, 980 (1995).
- <sup>19</sup> Y. Saiga and Y. Kuramoto, *J. Phys. Soc. Jpn.* **68**, 3631 (1999).
- <sup>20</sup> J. E. Hirsch and D. J. Scalapino, *Phys. Rev. B* **27**, 7169 (1983).
- <sup>21</sup> N. Nagaosa, *Solid State Commun.* **94**, 495 (1995).
- <sup>22</sup> H. J. Schulz, *Phys. Rev. B* **53**, R2959 (1996); in *Correlated Fermions and Transport in Mesoscopic Systems*, edited by T. Martin, G. Montambaux, and T. Trần Thanh Vân (Editions Frontières, Gif-sur-Yvette, France, 1996), p. 81.